A New Compact Paired-Parallel Architecture for Haptic Transparency

Margot Vulliez, Oussama Khatib

A new compact paired-parallel architecture for haptic transparency

Margot Vulliez and Oussama Khatib

Abstract This paper presents a highly compact paired-parallel mechanical architecture that aims for haptic transparency: accurate motion in free space and high force capability in contact. Low inertia and high stiffness of parallel manipulators are key properties to ensure force-motion fidelity in haptic applications. The proposed 7-DOF architecture combines two Delta-like translators in-parallel to a helical handle, to generate its translational and rotational motions with low coupling. The modeling of the architecture is simply written from the models of the Delta robots and the handle linkage. It shows that performances of such paired-parallel architecture derive from its components. A haptic device is designed based on this compact architecture. A prototype validates its mobility and the feasibility of the assembly.

1 Mechanical architectures for haptic transparency

Remote haptic interactions secure the human expert on an ergonomic workstation while taking advantage of the robot physical capabilities on site. The design of a high-fidelity haptic device is critical in teleoperation, since it forms the physical link between the operator and the remote environment. It captures the human gesture to be replicated by the remote robot. It provides sufficient sensory information to the user to remotely perform the task.

Fidelity of remote physical interactions can be assessed by haptic transparency: free space feels free; constraints feel rigid; solid objects persist [19]. A perfectly-transparent haptic system would reproduce the exact same impedance to the user than the one of the remote environment [16]. Several functional requirements must be met by the haptic device to be transparent. It must provide an unconstrained workspace, have low inertia, minimal joint clearance and low friction, to enable free and precise human motions. It must generate accurate and isotropic force feedback, within a large stiffness bandwidth, to the user to perceive the environment.

A dense state of the art proposes different kinematics of grounded general-purpose 6-DOF (Degrees Of Freedom) haptic devices. Although serial devices [18, 9, 6]) have simple kinematics with large workspace, the inherent flexibility and important inertia of their serial chain have a detrimental effect on transparency. Fully parallel structures [13, 15, 11] reflect low inertia and high stiffness to the user but suffer from complex modeling and a limited workspace, particularly in rotation.

Margot Vulliez
Auctus team, Inria, 33405 Talence, France, e-mail: margot.vulliez@inria.fr

Oussama Khatib
AI Lab, CS Dept, Stanford University, Stanford CA 94305, USA, e-mail: khatib@stanford.edu

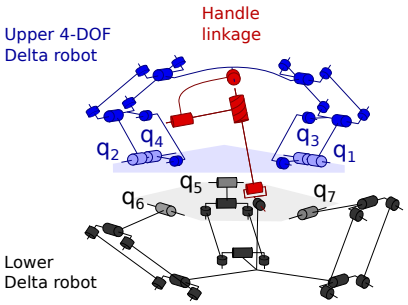

Fig. 1: New 7-DOF paired parallel kinematics

Devices which combine parallel and/or serial mechanisms together to generate 6-DOF motion make a good trade-off between their respective properties. Hybrid devices serially combine a serial wrist with a simple parallel architecture, such as a Delta-like [5, 1] or a Tripteron translator [10]. Paired-parallel architectures couple two simple mechanisms in-parallel to the end-effector. They can be composed of PHANToM-like five-bar linkages to provide a large workspace [7, 17, 22, 12]. But their serial chains do not provide comparable stiffness and accuracy than coupling parallel structures. Few paired-parallel devices combine two parallel mechanisms, such as two pantograph mechanisms [2] or two Delta robots [14, 20, 8].

The motivations of this work came from observations made on the Delthaptic [20] that we designed in the past. This paired-parallel 6-DOF haptic device is based on two Delta robots linked to a helical end-effector. It shows promising performances within a large workspace. It has a reasonable inertia and a fair stiffness thanks to its parallel mechanisms. It keeps a simple modeling. However, it suffers from a large and bulky structure, reducing its force capability, stiffness, and portability. This limitation supports a design revision to be highly compact, even at the expense of a reduced workspace. A compact architecture should have better dynamic performances and positioning accuracy. Efforts will also be done to ensure an easy and ergonomic use of device while the original design had a confined and difficult access to its handle.

This paper presents a highly compact paired-parallel architecture. It aims for haptic transparency (accurate motion, high and isotropic force capability, large stiffness bandwidth) thanks to a low-inertia and high-stiffness architecture.

2 A compact paired parallel architecture

2.1 Architectural concept

We propose a new compact paired-parallel architecture [21] to improve force-motion fidelity of haptic devices. This architecture is depicted in Figure 1. The lower Delta manipulator [4] (generalized coordinates q_5, q_6, q_7) is composed of three RRΠR legs for which the parallelograms constrain the mobile platform to translate. The upper redundant Delta4 manipulator [1] (q_1, q_2, q_3, q_4) is composed of two R(Π)RΠR legs

on which two rotary actuators (q_3, q_4) are added to control each leg second revolute joint through a parallelogram. Each parallelogram structure is made up of revolute joints, rather than the classical Delta spherical joints. This choice adds assembly constraints which: suppress the vertical rotational-DOF released by removing one of the three legs on the Delta4, or gained in the parallel singular configuration (all parallelograms coplanar to the platform plane); avoid constraint singularities in which the assembly constraint conferred by the parallelograms is lost (uncontrollable rotation of the classical Delta when two parallelograms are coplanar); and lead to an hyperstatic mechanical system that should be globally stiffer.

The two Delta-like robots are linked in-parallel to the two extremities of a helical handle to generate its translational (the two robots translate together) and rotational DOFs (the two robots have relative motions). To limit and better balance the inertial effects, the handle is attached to the upper robot at the center of a 3-DOF gyroscopic mechanism. A compact Universal joint, modified with a small axle-spacing to avoid interference, transmits the lower Delta motions to the handle bottom point.

High fidelity: The architecture preserves the benefits of parallel manipulators while providing 6-DOF mobility of the handle with low translational/rotational coupling: all actuators are grounded (low inertia), it combines parallel structures to generate large force, and it has simple models (easy to simulate and control).

Compact structure: Compactness is crucial to increase stiffness (accuracy) and to reduce effective inertia (force capability). The lower Delta robot has been turned upside down and the (q_3, q_4) transmission parallelograms have been placed inside the upper Delta envelope to reduce the device footprint and make it easily portable.

Accessibility: The upper Delta4, with only two legs, opens an access to the handle that can be secured with a crankcase, or made comfortable with a wrist holder.

2.2 Modeling

A major advantage of paired-parallel architectures is to preserve the properties of the manipulators it is composed of. The dynamic model of a parallel assembly is the sum of its components' dynamics [3]. Similarly we can express the kinematic model of the paired-parallel architecture as a combination of its components' kinematics.

Kinematic modeling

Given $\mathbf{q} = [\mathbf{q}_u, \mathbf{q}_l]^T \in R^{7\times1}$ the vector of generalized coordinates formed by the upper Delta4 (index u) active joints $\mathbf{q}_u = [q_1, q_2, q_3, q_4]^T$ and the lower Delta (index l) active joints $\mathbf{q}_l = [q_5, q_6, q_7]^T$, the Cartesian velocities $\dot{\mathbf{X}}_u = [\dot{x}_u, \dot{y}_u, \dot{z}_u]^T \in R^{3\times1}$ and $\dot{\mathbf{X}}_l = [\dot{x}_l, \dot{y}_l, \dot{z}_l]^T \in R^{3\times1}$ of the two mobile platforms can be expressed in the device task space $R_0(x_0, y_0, z_0)$ through the kinematic models:

$$\begin{aligned} \mathbf{A}_u\dot{\mathbf{X}}_u = \mathbf{B}_u\dot{\mathbf{q}}_u \;\text{ and }\; \mathbf{A}_l\dot{\mathbf{X}}_l = \mathbf{B}_l\dot{\mathbf{q}}_l \\ \mathbf{J}_u^{-1}\dot{\mathbf{X}}_u = \dot{\mathbf{q}}_u \;\text{ and }\; \mathbf{J}_l^{-1}\dot{\mathbf{X}}_l = \dot{\mathbf{q}}_l \end{aligned} \tag{1}$$

$$\mathbf{B}_u = \begin{bmatrix} \mathbf{B}_{u11} & \mathbf{B}_{u12} \\ \mathbf{B}_{u21} & 0_{2\times2} \end{bmatrix} = \begin{bmatrix} a_1 & 0 & b_1 & 0 \\ 0 & a_2 & 0 & b_2 \\ c_1 & 0 & 0 & 0 \\ 0 & c_2 & 0 & 0 \end{bmatrix} \;\text{ and }\; \mathbf{B}_l = \mathbf{diag}(B_{1l}, B_{2l}, B_{3l})$$

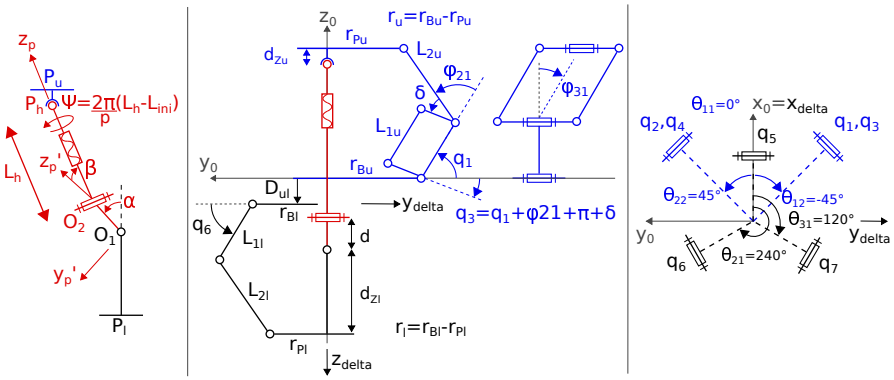

Fig. 2: Parameterization of the architecture

with $\mathbf{A}_u \in R^{3\times4}$ and $\mathbf{A}_l \in R^{3\times3}$ the parallel kinematic Jacobian matrices and $\mathbf{B}_u \in R^{4\times4}$ and $\mathbf{B}_l \in R^{3\times3}$ the serial kinematic Jacobian matrices. Parallel singular configurations are reflected by $det(\mathbf{A_l}) = 0$ and $det(\mathbf{A_u}^T\mathbf{A_u}) = 0$ and the forward kinematic models have 2 solutions (assembly modes), resp. the external position ($det(\mathbf{A}) < 0$) or the internal position ($det(\mathbf{A}) > 0$) of the platform. Serial singular configurations are reflected by $det(\mathbf{B_l}) = 0$ and $det(\mathbf{B_u}) = 0$. The Delta Inverse Kinematic Model (IKM) has 8 solutions (working modes), internal ($B_{jl} > 0$) or external ($B_{jl} < 0$) configurations of each leg $j = [1, 2, 3]$. The Delta4 IKM has 4 solutions, internal ($c_j > 0$) or external ($c_j < 0$) configurations of each leg $j = [1, 2]$.

If we, then, consider the two kinematic linkages between the Delta platforms and the helical handle, with respect to the parameterization given in Figure 2, the translational velocity decomposition from the points P_u to P_l gives:

$$L_h\mathbf{z}_p \times \boldsymbol{\omega}_{h/0} = \dot{\mathbf{X}}_l - \dot{\mathbf{X}}_u - \dot{\alpha}d\mathbf{y}'_p + \dot{L}_h\mathbf{z}_p = \mathbf{V} \tag{2}$$

$\boldsymbol{\omega}_{h/0}$ denotes the rotational velocity of link h with respect to the world frame R_0. Indices u, l, h, s, c resp. designate the upper Delta, the lower Delta, the handle body, the screw of the helical joint, the cardan shaft of the U-joint.

Equation (2) can be solved as the sum of a particular solution $\boldsymbol{\omega}^0_{h/0}$ and the velocity term colinear to $\mathbf{z}_p$ given by the helical joint equation:

$$\boldsymbol{\omega}_{h/0} = \boldsymbol{\omega}^0_{h/0} + \lambda\mathbf{z}_p = \frac{\mathbf{V} \times L_h\mathbf{z}_p}{L_h^2} + \frac{2\pi}{p}\dot{L}_h\mathbf{z}_p \tag{3}$$

From Eq.(3), the task space velocity $\dot{\mathbf{X}} = [\dot{x}, \dot{y}, \dot{z}, \omega_x, \omega_y, \omega_z]^T \in R^{6\times1}$ of the paired-parallel architecture can be computed from the two Delta robots' kinematics and their linkages to the handle described by the coupling Jacobian matrix $\mathbf{J}_c \in R^{6\times6}$:

$$\dot{\mathbf{X}} = \begin{bmatrix}\mathbf{J}_{cu} & \mathbf{J}_{cl}\end{bmatrix}\begin{bmatrix}\dot{\mathbf{X}}_u \\ \dot{\mathbf{X}}_l\end{bmatrix} = \mathbf{J}_c\begin{bmatrix}\mathbf{J}_u & 0_{3\times3} \\ 0_{3\times4} & \mathbf{J}_l\end{bmatrix}\dot{\mathbf{q}} = \mathbf{J}\dot{\mathbf{q}} \tag{4}$$

This full forward kinematic model shows that kinematic properties and singularities of the paired parallel architecture are given by a simple kinematic analysis of the Delta robots and the handle kinematic chain.

Dynamic modeling

Given the joint torque vector $\boldsymbol{\tau} = [\boldsymbol{\tau}_u, \boldsymbol{\tau}_l]^T \in R^{7\times1}$, formed by the upper Delta4 joint torques $\boldsymbol{\tau}_u = [\tau_1, \tau_2, \tau_3, \tau_4]^T$ and the lower Delta joint torques $\boldsymbol{\tau}_l = [\tau_5, \tau_6, \tau_7]^T$, the task forces $\mathbf{F}_u$ and $\mathbf{F}_l \in R^{3\times1}$ generated by each platform can be computed by the two dynamic models of the Delta robots in operational space:

$$\begin{aligned} \boldsymbol{\Lambda}_u\ddot{\mathbf{X}}_u + \boldsymbol{\mu}_u + \mathbf{p}_u &= \mathbf{F}_u = \mathbf{J}_u^{-T}\boldsymbol{\tau}_u \\ \boldsymbol{\Lambda}_l\ddot{\mathbf{X}}_l + \boldsymbol{\mu}_l + \mathbf{p}_l &= \mathbf{F}_l = \mathbf{J}_l^{-T}\boldsymbol{\tau}_l \\ \text{with } \boldsymbol{\Lambda}_i = \sum_j \boldsymbol{\Lambda}_{ij} + \boldsymbol{\Lambda}_{ip};\ \boldsymbol{\mu}_i = \sum_j \boldsymbol{\mu}_{ij} + \boldsymbol{\mu}_{ip};\ \mathbf{p}_i &= \sum_j \mathbf{p}_{ij} + \mathbf{p}_{ip} \end{aligned} \tag{5}$$

where $\boldsymbol{\Lambda}_u$ and $\boldsymbol{\Lambda}_l \in R^{3\times3}$, $\boldsymbol{\mu}_u(\mathbf{X}_u, \dot{\mathbf{X}}_u)$ and $\boldsymbol{\mu}_l(\mathbf{X}_l, \dot{\mathbf{X}}_l) \in R^{3\times1}$, and $\mathbf{p}_u(\mathbf{X}_u)$ and $\mathbf{p}_l(\mathbf{X}_l) \in R^{3\times1}$ are respectively the inertia matrices, the Coriolis and centrifugal force vectors, and the gravity terms in operational space. We see from Eq. (5) that the dynamic model of each Delta robot i can be computed as the sum of the platform inertia $\boldsymbol{\Lambda}_{ip}$, Coriolis and centrifugal $\boldsymbol{\mu}_{ij}$, and gravity $\mathbf{p}_{ij}$ terms and the legs j inertia $\boldsymbol{\Lambda}_{ij} = \mathbf{J}_{ij}^{-T}\mathbf{A}_{ij}\mathbf{J}_{ij}^{-1}$, Coriolis and centrifugal $\boldsymbol{\mu}_{ij} = \mathbf{J}_{ij}^{-1}\mathbf{b}_{ij} - \boldsymbol{\Lambda}_{ij}\dot{\mathbf{J}}_{ij}\dot{\mathbf{q}}_{ij}$, and gravity $\mathbf{p}_{ij} = \mathbf{J}_{ij}^{-1}\mathbf{g}_{ij}$ terms in operational space. Here $\mathbf{J}_{ij}$, $\mathbf{A}_{ij}$, $\mathbf{b}_{ij}$, and $\mathbf{g}_{ij}$ are the leg j kinematic Jacobian matrix, the inertia matrix, the Coriolis and centrifugal effect, and the gravity torque vector in the leg joint space.

We can, then, apply the augmented-object theory to the paired parallel architecture, as it combines the two Delta robots in-parallel to the end-effector, to compute the generalized operational force vector $\mathbf{F}_\oplus = [\mathbf{F}, \boldsymbol{\Gamma}]^T \in R^{6\times1}$:

$$\begin{aligned} \boldsymbol{\Lambda}_\oplus\ddot{\mathbf{X}} + \boldsymbol{\mu}_\oplus + \mathbf{p}_\oplus &= \mathbf{F}_\oplus = \mathbf{J}^{-T}\boldsymbol{\tau} \\ \text{with } \boldsymbol{\Lambda}_\oplus = \mathbf{J}_c^{-T}\begin{bmatrix} \boldsymbol{\Lambda}_u & 0_{3\times3} \\ 0_{3\times4} & \boldsymbol{\Lambda}_l \end{bmatrix}\mathbf{J}_c^{-1} + \boldsymbol{\Lambda}_h;\ \mathbf{p}_\oplus &= \mathbf{J}_c^{-T}\begin{bmatrix} \mathbf{p}_u \\ \mathbf{p}_l \end{bmatrix} + \mathbf{p}_h; \\ \boldsymbol{\mu}_\oplus = \mathbf{J}_c^{-T}\begin{bmatrix} \boldsymbol{\mu}_u \\ \boldsymbol{\mu}_l \end{bmatrix} - (\mathbf{J}_c^{-T}\begin{bmatrix} \boldsymbol{\Lambda}_u & 0_{3\times3} \\ 0_{3\times4} & \boldsymbol{\Lambda}_l \end{bmatrix}\mathbf{J}_c^{-1})\dot{\mathbf{J}}_c\begin{bmatrix} \dot{\mathbf{X}}_u \\ \dot{\mathbf{X}}_l \end{bmatrix} &+ \boldsymbol{\mu}_h \end{aligned} \tag{6}$$

The dynamic model (6) of the paired parallel architecture simply expresses the operational-space inertia matrix $\boldsymbol{\Lambda}_\oplus \in R^{6\times6}$, Coriolis and centrifugal effects $\boldsymbol{\mu}_\oplus \in R^{6\times1}$ and gravity force vector $\mathbf{p}_\oplus \in R^{6\times1}$ based on the dynamical components of the two Delta robots (5), the coupling Jacobian matrix $\mathbf{J}_c$ (4), and the inertia matrix $\boldsymbol{\Lambda}_h$, the Coriolis and centrifugal vector $\boldsymbol{\mu}_h$, and the gravity force $\mathbf{p}_h$ from the handle h. It gives a simple and analytical equation to study the effective dynamics of a device with such a paired parallel architecture, and it makes it easy to compute the command joint torques $\boldsymbol{\tau}^*$ required to generate a desired haptic feedback.

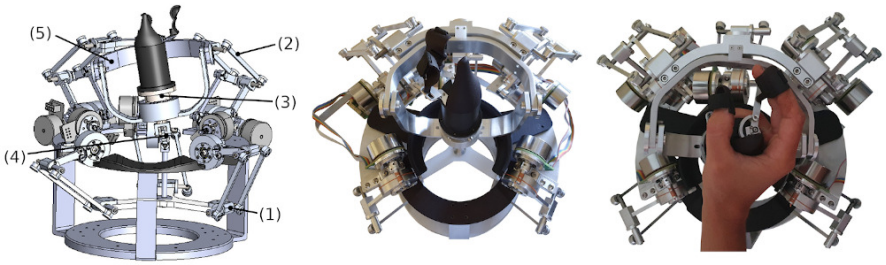

Fig. 3: Prototype of the haptic device: (1) lower Delta robot, (2) upper Delta4 robot, (3) helical handle, (4) modified U-joint, (5) 3-DOF gyroscopic mechanism.

3 Design of the compact haptic device

The compact 7-DOF paired-parallel architecture forms the kinematic basis of a new haptic device. It helps to gain stiffness, to reduce effective inertia, and therefore to increase the device force-motion fidelity. We briefly outline the design methodology we used to develop the haptic device and describe the developed prototype.

Design optimization: A constrained multi-objective optimization process is run to select optimal structural and actuation parameters with respect to desired performances. It provides a set of solutions defined by their design parameters. They verify all design constraints and aims at both maximizing kinematic capability (cost that maximizes the operational-space velocity) and dynamic capability (cost that maximizes the task force and minimizes inertia, Coriolis and gravity terms).

Design constraints: Different design constraints have been defined in terms of workspace, singular configurations, and expected dynamic capabilities to convey functional requirements. We set kinematic constraints: a maximum joint range of motion $-\pi < q_a < \pi/2$ to avoid link interference; a $\pm 25mm \times \pm 20°$ prescribed workspace must be reachable; no singular configuration in the workspace ($det(\mathbf{A}_u) \neq 0$, $det(\mathbf{B}_u) \neq 0$, $det(\mathbf{A}_l) \neq 0$, $det(\mathbf{B}_l) \neq 0$, $det(\mathbf{J}_c) \neq 0$); the external assembly modes ($det(\mathbf{A_l}) < 0$ and $det(\mathbf{A_u}) < 0$) and the external working modes ($B_{jl} < 0$ and $c_j < 0$) for the Delta robots; the device volume must stay under a maximum footprint for compactness $r_{max} = max(L_{1u}, L_{1l}) \leq 100m$ and $h_{max} = L_{1u} + L_{2u} + L_{1l} + L_{2l} \leq 400m$. We add dynamic constraints to ensure minimum device performances: a static haptic force $F_{max} \geq 20N$ and torque $\Gamma_{max} \geq 0.5Nm$ in all direction (isotropic capability) given the nominal torque $T_{nom} = 0.134Nm$ of the selected motors and $\tau_{max,i} = T_{nom}/R_i$ with R_i the joint i transmission ratio; a permissible motor-to-joint inertia ratio $I_{eq,i}/20 < I_{mot} = 181gcm^2$ with $I_{eq,i} = R_i^2 A_{\oplus,ii}$ the effective inertia projected on the axis of the actuator i. The joint space inertia matrix is $\mathbf{A}_\oplus = J^T \mathbf{\Lambda}_\oplus J$.

Design parameters: The design parameters (see Fig.2) are the geometric structural parameters (legs' length, platforms' radius, handle linkage distances), the height H of the workspace center with respect to the world frame, and transmission parameters (actuated joint transmission ratio and screw pitch of the helical handle): $D = (L_{1u}, L_{2u}, r_u, dzu, L_{1l}, L_{2l}, r_l, dzl, D_{ul}, H, d, R_{1u}, R_{2u}, R_l, p)$.

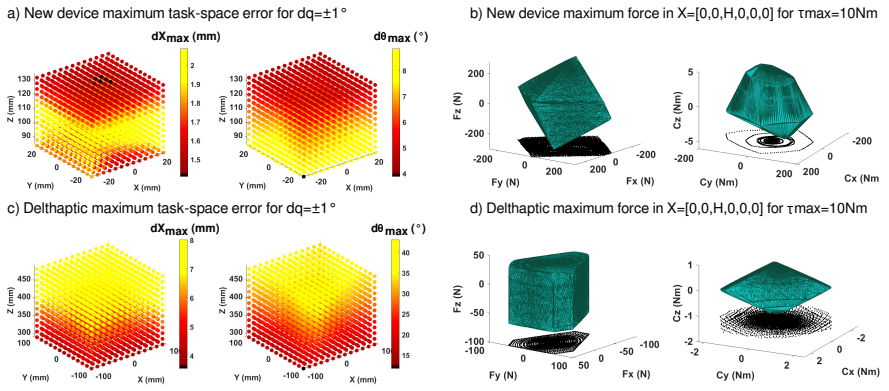

Fig. 4: Position accuracy and force capability for the new device and the Delthaptic

Prototype: The optimization process gives the design parameters in mm $D = (71, 92, -25, 9.5, 72, 101, 5, 81, -12, 110, 16, 1/10, 1/10, 1/10, 120)$. After a full definition of each part topology, each joint bearing assembly, the cable-based capstan transmission system, the helical handle, and the integration of the motors, a prototype of the haptic device was manufactured, as depicted in Fig. 3. It validates the chosen assembly and demonstrate expected mobility of the device. We are currently evaluating the prototype performances to validate or refine the design choices.

Performances: Simulated performances of the new device and the Delthaptic are compared in Fig. 4. As expected, the compactness of the new device highly increases its force capability and positioning accuracy. Plots a) and c) give the maximum position error in operational space $\mathbf{dX}_{max}$ that results from joints' clearance $\mathbf{dq} = \pm 1°$. This error stays below $2.1mm$ and $9°$ along the new device workspace while it reaches $8mm$ and $44°$ for the Delthaptic. The operational-space force capability is given in b) and d) at the center of the workspace. It is computed from the static model such as $-[\boldsymbol{\tau}_{max}] - \mathbf{J}^T\mathbf{p}_{\oplus} \leq \mathbf{J}^T\mathbf{F}_{\oplus} \leq [\boldsymbol{\tau}_{max}] - \mathbf{J}^T\mathbf{p}_{\oplus}$. For comparison purpose, we consider the same maximum joint torques of $\tau_{max} = 10Nm$ for both devices. The new device can produce a force about $200N$ in all direction of the task space while the Delthaptic can only generate about $50N$ in the (x, y) axes and $100N$ in the z axis. Similarly, the torque capability of the new device is about $5Nm$ versus $1Nm$ for the Delthaptic in the z axis and about $200Nm$ versus $2Nm$ in the (x, y) axes. Therefore, the new architecture presents a high force capability which is quasi-isotropic, expect the torque around the handle's axis (z in the plotted configuration) for which the ball-screw system reduces the force transmission ratio.

4 Conclusion

We have presented a highly compact paired-parallel architecture that combines an upper redundant Delta4 robot and a lower Delta robot in-parallel to a helical handle. It generates the 6-DOF motion of the end-effector while maintaining the high stiffness

and low inertia properties of parallel manipulators. This very compact mechanical architecture increases haptic transparency, through a high-fidelity quasi-isotropic dynamic behavior in force/motion. A haptic device with this architecture was designed, optimized, and prototyped to validate the proposed concept.

Compactness of the device is crucial to increase haptic transparency, but it requires to reduce its operational workspace. Workspace mapping strategies, that will be presented in future works, have been developed to counteract this small workspace.

References

1. Arata, J., Kondo, H., Ikedo, N., Fujimoto, H.: Haptic device using a newly developed redundant parallel mechanism. IEEE Transactions on robotics **27**(2), 201–214 (2011)
2. Bassan, H., Talasaz, A., Patel, R.V.: Design and characterization of a 7-dof haptic interface for a minimally invasive surgery test-bed. In: 2009 IEEE/RSJ IROS, pp. 4098–4103 (2009)
3. Chang, K.S., Holmberg, R., Khatib, O.: The augmented object model: Cooperative manipulation and parallel mechanism dynamics. In: 2000 IEEE ICRA, vol. 1, pp. 470–475 (2000)
4. Clavel, R.: Delta, a fast robot with parallel geometry. In: Int. Symp. on Industrial Robot (1988)
5. Conti, F., Grange, S., Helmer, P., Rouiller, P.: Force-feedback device and method. (U.S. Patent Application No 12/228,260, 11 févr. 2010)
6. Garrec, P., Friconneau, J.P., Louveaux, F.: Virtuose 6d: A new force-control master arm using innovative ball-screw actuators. In: ISR 35th International Symposium on Robotics (2004)
7. Gosselin, F., Ferlay, F.: Robot or haptic interface structure with parallel arms (2015). US Patent 8,950,286
8. Harada, T., Yase, H.: Family of six-dof novel two-platform parallel robots and development of re-configurable prototypes. In: 2023 IEEE ROBIO, pp. 1–6 (2023)
9. Hayward, V., Gregorio, P., et al.: Freedom-7: A high fidelity seven axis haptic device with application to surgical training. In: Experimental Robotics Symposium, pp. 443–456 (1998)
10. He, R., Zhang, B., Bi, Z., Zhang, W.: Development of a hybrid haptic device with high degree of motion decoupling. In: 2022 28th IEEE M2VIP, pp. 1–5 (2022)
11. Jin, L., Duan, X., Li, C., Shi, Q., Wen, H., Wang, J., Li, H.: Design of a novel parallel mechanism for haptic device. Journal of Mechanisms and Robotics **13**(4), 045001 (2021)
12. Kang, L., Yang, Y., Yi, B.J.: Design and implementation of a two-limbed 3t1r haptic device. In: 2023 IEEE/RSJ IROS, pp. 467–472 (2023)
13. Khan, S., Ahmad, A., Andersson, K.: Design optimization of the tau haptic device. In: 2011 3rd IEEE ICUMT, pp. 1–8 (2011)
14. Lallemand, J.P., Goudali, A., Zeghloul, S.: The 6-dof 2-delta parallel robot. Robotica **15**(4), 407–416 (1997)
15. Lambert, P., Herder, J.L.: A 7-dof redundantly actuated parallel haptic device combining 6-dof manipulation and 1-dof grasping. Mechanism and Machine Theory **134**, 349–364 (2019)
16. Lawrence, D.A.: Stability and transparency in bilateral teleoperation. IEEE transactions on robotics and automation **9**(5), 624–637 (1993)
17. Lee, G., Hur, S.M., Oh, Y.: High-force display capability and wide workspace with a novel haptic interface. IEEE/ASME Transactions on Mechatronics **22**(1), 138–148 (2016)
18. Massie, T.H., Salisbury, J.K., et al.: The phantom haptic interface: A device for probing virtual objects. In: ASME Symposium on HIVETS, vol. 55, pp. 295–300 (1994)
19. Salisbury, K., Brock, D., Massie, T., et al.: Haptic rendering: Programming touch interaction with virtual objects. In: 1995 symposium on Interactive 3D graphics, pp. 123–130 (1995)
20. Vulliez, M., Zeghloul, S., Khatib, O.: Design strategy and issues of the delthaptic, a new 6-dof parallel haptic device. Mechanism and Machine Theory **128**, 395–411 (2018)
21. Vulliez, M.R., Khatib, O.: Compact paired parallel architecture for high-fidelity haptic applications (2023). US Patent App. 18/022,208
22. Wen, K., Nguyen, T.S., Harton, D., Laliberté, T., Gosselin, C.: A backdrivable kinematically redundant (6+3)-degree-of-freedom hybrid parallel robot for intuitive sensorless physical human-robot interaction. IEEE Transactions on Robotics **37**(4), 1222–1238 (2020)